Colloids and Surfaces A: Physicochemical and Engineering Aspects 676 (2023) 132104

Contents lists available at ScienceDirect

Colloids and Surfaces A: Physicochemical and Engineering Aspects

journal homepage: www.elsevier.com/locate/colsurfa

Effects of zeta-potential on enhanced removal of hexavalent chromium by polypyrrole-*graft*-chitosan biodegradable copolymer

Mehmet Cabuk [a,*], Murat Oztas [b], Fethiye Gode [b], Halil Ibrahim Unal [c], Mustafa Yavuz [b]

[a] *Metallurgical and Material Engineering Department, Engineering Faculty, Mersin University, Mersin, Turkiye*
[b] *Chemistry Department, Sciences Faculty, Süleyman Demirel University, Isparta, Turkiye*
[c] *Chemistry Department, Science Faculty, Smart Materials Research Lab., Gaz i University, Ankara, Turkiye*

HIGHLIGHTS

- Cr(VI) ions adsorptions of biodegradable PPy-*g*-CS was found to change with changing the ζ-potential of the solutions.
- The initial ζ-potential of PPy was increased significantly from +14 mV to +47 mV at pH of 4.8 after grafting with CS chains.
- Maximum Cr(VI) removal was 73% for PPy, whereas, it was enhanced to 98% for PPy-*g*-CS copolymer at pH of 4.8 and 25 °C.
- The PPy-*g*-CS copolymer with high ζ-potential (128 mg/g at pH of 4.8) would be a good adsorbent candidate.

GRAPHICAL ABSTRACT

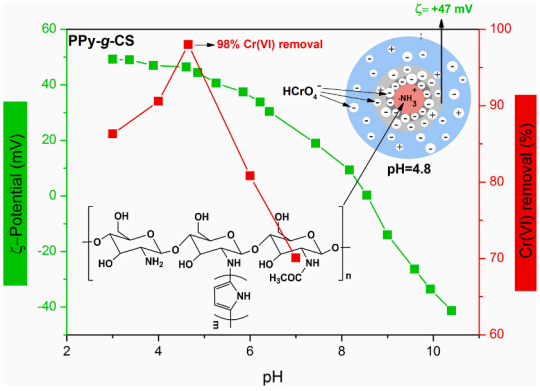

ARTICLE INFO

Keywords:
Zeta potential
Polycationic chitosan
Polypyrrole
Graft copolymer
Chromium removal
Water pollution

ABSTRACT

In the present research, chitosan grafted polypyrrole (PPy-*g*-CS) biodegradable copolymer particles were used as novel adsorbent to remove hexavalent chromium ions, Cr (VI), from water solutions and compared with the PPy. The effects of zeta (ζ)-potentials of these nanoparticles on the uptake properties of Cr(VI) ions were investigated as a function of pH. It was observed that the ζ-potential of PPy was shifted significantly from + 14 mV ($pH_{initial}$=4.8 for PPy) to + 47 mV ($pH_{initial}$=4.8 for PPy-*g*-CS) owing to the covalently grafting of polycationic CS chains with PPy chains. Thus, effective sites ($-NH_3^+$)for adsorption of Cr(VI) ions were created at the surfaces of the substrate. Adsorption efficiency of the PPy-*g*-CS copolymer observed to change by changing the pH of the medium which resulted in the variation of ζ-potential. The uptake capability of the PPy-*g*-CS copolymer increased compared to the pristine PPy. The maximum removal of Cr(VI) at the optimum pH of 4.8 and at 25 °C was 98 % and 73 % for PPy-*g*-CS and PPy, respectively. The adsorption kinetics was pseudo-second-order and inconsistent with the Freundlich isotherm. According to the thermodynamic parameters, the adsorption was endothermic ($\Delta H^\circ_{PPy\text{-}g\text{-}CS}$ = 7.12 kJ/mol), spontaneous ($\Delta G^\circ_{PPy\text{-}g\text{-}CS}$ = −546.43 kJ/mol) and driven by the increased entropy ($\Delta S^\circ_{PPy\text{-}g\text{-}CS}$ = 247.55 J/mol.K) of the system. In conclusion, the biodegradable PPy-*g*-CS graft copolymer particles with enhanced positive ζ-potential (+47 mV at pH=4.8) and adsorption capability (128 mg/g) would be a

* Correspondence to: Metallurgical and Material Engineering Department, Faculty of Engineering, Mersin University, Çiftlikköy, Mersin, Turkiye.
E-mail addresses: mehmetcabuk@mersin.edu.tr, mhmtcbk@gmail.com (M. Cabuk).

https://doi.org/10.1016/j.colsurfa.2023.132104
Received 9 February 2023; Received in revised form 9 June 2023; Accepted 18 July 2023
Available online 20 July 2023

good candidate as an environmentally friendly adsorbent for the removal of negatively charged pollutants from water resources.

1. Introduction

Pollution of water resources caused by toxic heavy metal cations (i.e., Pb^{2+}, Cd^{2+}, Cr^{6+}, Hg^{2+}, Cu^{2+}, etc.) has turned into a very dangerous environmental issue in the recent years which put the health of the living species in danger [1]. Among these heavy metals, chromium (Cr) is a serious pollutant commonly released by the industrial sites such as metal plating, pigment production, mining, tannery and textile [2]. Although chromium transforms into several different oxidation states, Cr(III) and Cr(VI) are the most stable forms in nature [3]. Cr(III) has limited ionic mobility due to the small value of K_{sp} (1.6×10^{-30} at 25 °C) of $Cr(OH)_3$ which is the most stable form of Cr(III) ions in nature. This slightly soluble property makes the Cr(III) ions genetically less toxic. In contrast, Cr(VI) ions primarily exist as in the form of $HCrO_4^-$ and CrO_4^{2-} with high solubility in water which increases their mobility and so the toxicity in biological systems. Therefore, the efficient removal of Cr(VI) from water resources has become an important issue to overcome and concern of the researchers [4]. That is why its maximum allowable level for total chromium is set to be less than 0.05 $mg{\cdot}L^{-1}$ in drinking-water by the World Health Organization (WHO) [5].

To remove these chromium ions from waste water resources, various methods such as ion exchange, ultrafiltration and reverse osmosis are currently in use [6–8]. However, these methods have generally high cost, low efficiency and drawbacks especially for very dilute solutions. Adsorption is widely used physicochemical separation method for the removal of pollutants from wastewater due to its easy operation, high efficiency and low cost [9,10].

Recently, nanomaterials are proposed for adsorption processes of heavy metals from waste water with enhanced adsorption capacity, sorption rate, high surface area, big aspect ratio, fast diffusion rate, high upcycling capacity and functional active sites readily available on their chemical structures [11]. Therefore, it is expected to produce advanced nano adsorbents that can uptake large amounts of Cr(VI) from waste water.

In recent years for this purpose, the removals of anionic metal oxide pollutants through the electrostatic interactions of amino functionalized materials have attracted great attention [12]. Chitosan (CS) is a biopolymer containing functional free amino groups (-NH_2) with amino polysaccharide structure. Their amino groups are protonated under acidic conditions and turn into a polycationic structure ($-NH_3^+$) and easily interact with the anions [13,14]. Functional CS has been investigated as a potential bio-based and environmentally friendly adsorbent for metal oxide anions from waste water solutions by chelating heavy metals with amino and hydroxyl groups [15]. The drawbacks of CS are low surface area, weak mechanical properties and solubility difficulties in highly acidic solutions, which limits its application in adsorption processes [16,17]. To overcome these drawbacks of CS, some chemical and physical modifications are reported in the literature. For example, various graft copolymers such as chitosan-*g*-*n*-butylacrylate [18], chitosan-*g*-chloroacetic acid [19] and chitosan-*g*-itaconic acid [20] are fabricated and used as adsorbents for various heavy metals.

On the other hand, it has been reported in the literature that conductive polymers are highly effective adsorbents in removing Cr(VI) ions [21]. Polypyrrole (PPy) is one of the most important conductive polymers with many advantages such as easy synthesis, adjustable electrical conductivity, and environmental stability [22]. It is well known that PPy undergoes to protonation and deprotonation processes by changing its surface charges when subjected to doping and dedoping cycles in basic or acidic conditions, respectively [23].

Determination of the electrokinetic properties of dispersed solid particles are carried out by measuring their ζ-potentials. The ζ-potential of a solution changes depending on pH, ionic strength, valency of the ions and temperature of the medium. In a dispersion it is possible to gather information on the colloidal stability, surface charges, electrical double layer and interactions between the dispersed and dispersing interfaces by the ζ-potential measurements [24,25].

To the best of our knowledge, effect of ζ-potential on the adsorption behavior of Cr(VI) ions onto functional PPy-*g*-CS graft copolymer dispersions has not hitherto been reported and discussed in the literature. That is why a novel study is carried out to investigate the effects of ζ-potential change on the adsorption yield of Cr(VI) ions from water solutions as functions of pH, adsorbent concentration, contact time of ions with the adsorbent, temperature of the medium and surface charges. Further, kinetic and thermodynamic parameters are revealed and compared with the pristine PPy and discussed with the literature.

2. Experimental

2.1. Materials

Pyrrole (99 % pure), chitosan, (medium molecular weight and 75–82 % deacetylation degree), $FeCl_3.6\ H_2O$ (97 % pure), $K_2Cr_2O_7$, HCl and NaOH were analytical grade, obtained from Merck (Germany) and used as received. The pH values of the dispersions were adjusted by using 0.25 M HCl(aq) and 0.25 M NaOH(aq). Other chemical materials used were obtained from Aldrich company in analytical grade and used as received.

2.2. Synthesis of PPy-g-CS copolymer

PPy-*g*-CS copolymer was synthesized by chemical oxidative radical polymerization method using $FeCl_3 0.6\ H_2O$ initiator in acidic medium. The PPy particles were functionalized with CS to increase the number of available adsorption sites ($-NH_3^+$), surface charge, colloidal stability and consequently the adsorption capacity. PPy-*g*-CS graft copolymer particles were characterized by means of FTIR, ^{1}H NMR, TGA, SEM, TEM, and UV–VIS techniques. The grafting yield, grafting efficiency, particle size, dielectric constant and density of the conducting graft copolymer were determined and details on the synthesis, characterization and grafting mechanism of the PPy-*g*-CS graft copolymer were presented extensively in our previous publication [26]. In this study, effects of ζ -potential and pH on Cr(VI) adsorption of the PPy-*g*-CS graft copolymer were investigated.

2.3. Determination of physical properties

All the samples were dried and ground milled in order to reduce the particle size and provide a homogeneous size distribution. The details of the results obtained on some physical properties of the samples (i.e., hydrodynamic particle size, and apparent density) are explained in our previous study [26].

2.4. Electrokinetic measurements

Malvern Zeta-sizer Nano ZS device operating according to the Laser Doppler Electrophoresis technique was used for the ζ-potential measurements of PPy-*g*-CS copolymer aqueous dispersions. The ζ-potential is determined from the electrophoretic mobility of the dispersed particles by using the Henry's Eq. (1):

$$\zeta = \frac{3\eta U_E}{2\varepsilon f(\kappa\alpha)} \tag{1}$$

where η is the viscosity of the medium (N m^{-2} s), U_E is the electrophoretic mobility (m^2 V^{-1} s^{-1}), ε is permittivity of the medium (F m^{-1}), and $f(\kappa\alpha)$ is the Henry's function, κ is the Debye length (m^{-1}), and α is the radius of the particle (m). In order to study the effect of pH on the ζ-potential of PPy-*g*-CS colloidal particles, 0.1 g/L colloidal dispersion was prepared in 1.0×10^{-3} M NaCl(aq). The dispersion prepared at room temperature was sonicated for 30 min and rested for 2 h to establish a kinetic equilibrium. All the measurements were performed in the pH range of 3–11 at 25 ºC. The pH measurement of the dispersion was performed immediately by using an MPT-2 auto titration unit.

2.5. Adsorption experiments

Adsorption experiments of PPy and PPy-*g*-CS samples were carried out by using a batch technique at 25 °C. For this purpose, the experiments were carried out in bottles containing distilled water (25 mL) and stirred at 250 rpm in a shaker. The Cr(VI) concentration varied from 1.0×10^{-4} to 1.0×10^{-3} M by using $K_2Cr_2O_7$. The pH values of the dispersions were adjusted in the range of 2–7. After equilibration time of 2 h, the bottles were taken from the shaker and the dispersions were filtered. Residual Cr(VI) content of the supernatant liquids on each bottle were determined by atomic absorption spectroscopy (Perkin Elmer model AA800, USA). The effect of adsorbent dosage on the adsorption yield was investigated at a dose range of 0.01 g (0.4 g/L) to 0.5 g (20 g/L) and the concentration of Cr(VI) was 1.0×10^{-3} M for each dispersion. Effect of temperature on the adsorption performance was investigated in the range of 25–65 °C using a thermostatic shaking water bath (Memmert WB29 model, Germany). The pH values were measured with a pH meter (Eutech Instruments Ion 510 model, USA). The adsorbed Cr(VI) amounts (qe, mg/g) were determined via Eq. (2).

$$q_e = \frac{(C_o - C_e)V}{m} \tag{2}$$

where C_o and C_e are the initial and equilibrium concentrations of Cr(VI) ions (in mg/L), respectively, m is the mass of adsorbent (g) and V is the volume of solution (L). The percent of Cr(VI) removal was calculated by Eq. (3).

$$Removal(\%) = \frac{(C_o - C_e)100}{C_o} \tag{3}$$

Finally, in order to determine the reusability of the adsorbent, the cyclic adsorption properties of PPy-*g*-CS graft copolymer for Cr(VI) were studied by five consecutive adsorption-desorption processes. For this purpose, 0.5 mg adsorbent was mechanically mixed at 60 rpm for 2 h in 40 mL of Cr(VI) solution having concentration of 100 mg/L and the pH of 4.8. The Cr(VI)-loaded adsorbent was filtered and washed with distilled water several times. Then, 0.01 M, 5 mL NaOH solution was added and mixed for 1 h at room temperature. Desorption processes took place in NaOH solution by exchanging OH^- ions with adsorbed $HCrO_4^-$ ions. Further, the upcycled adsorbent was dried at 60 °C for 24 h, and the same procedure was repeated for each cycle.

3. Results and discussions

3.1. Determination of the physical properties

SEM image of PPy-*g*-CS particles exhibited spherical, poor monodispersity and agglomerated morphologies (Fig. 1a). The hydrodynamic particle size of PPy was 140 nm, it was increased to 180 nm after grafting on polycationic functional CS chains (Fig. 1b). Similar particle size increase was reported for PPy/monodisperse latex spheres (MLS) in the literature. While the MLS possessed uniform particle size of 226 nm, PPy/MLS composite also possessed sphericity but poor monodispersity with an average hydrodynamic diameter of 255 nm [4]. Apparent density of the PPy was observed to decrease from 0.93 g/cm^3 to 0.88 g/cm^3, as expected, after grafting with low density CS chains which also cause steric hindrance on the PPy surface to increase the total volume.

These results further confirmed that PPy chains were successfully grafted onto CS back-bone. As grafting mechanism, pyrrole radicals may be ascribed to attack to the saccharide units of CS. During the grafting reaction, both grafting yield and grafting efficiency values raised with time, due to the increased amounts of formed PPy macro radicals on the saccharide units of CS. The reduced monomer and free pyrrole radicals in the reaction system led to the leveling off of grafting parameters with increasing reaction time. These results are in accordance with the study reported by Lee et al. which is on suspensible CS-PPy composite [27].

3.2. Effect of pH on ζ-potential

Solution pH is a very important factor that affects the ζ-potential and adsorption process. The ζ-potential of a particle in suspension can be defined as the electrical potential at the interface which separates the fluid that remains attached to the surface of the particle from the rest of the mobile fluid [28]. As shown in Fig. 2a, the PPy-*g*-CS particles exhibited a positive ζ-potential of + 47 mV at the initial equilibrium pH of 4.8. This value indicates that the particles are colloidally highly stable in the dispersion. The ζ-potential of the PPy-*g*-CS particles changed in the range of + 49 mV≥ ζ ≥ −44 mV at the pH range of 3–11 and the isoelectric point (IEP) was observed at the pH of 8.4. The initial pH of the pristine CS biopolymer was 5.8. As the pH changed between 3 and 11,

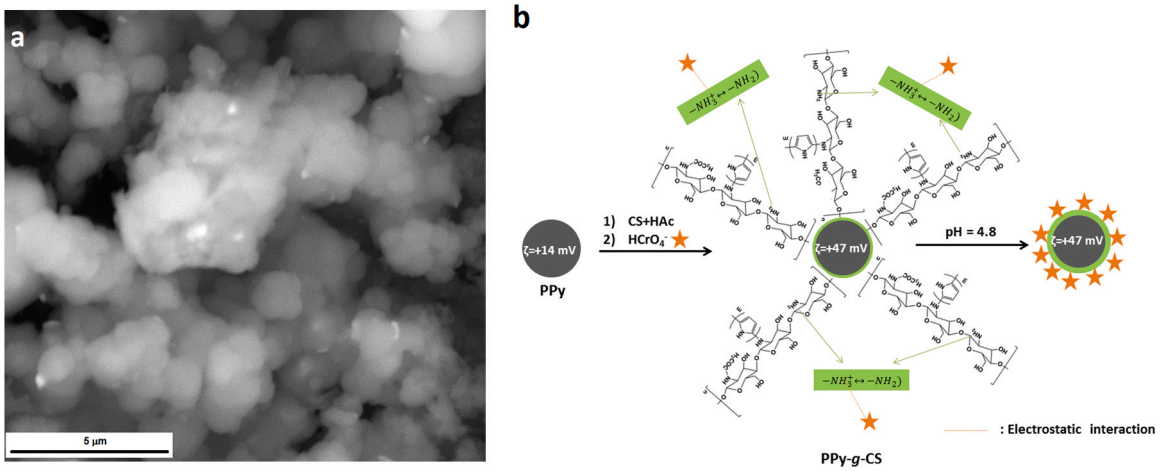

Fig. 1. (a) SEM image of the PPy-*g*-CS particles; (b) Schematic mechanism of Cr(VI) adsorption on positively charged PPy-*g*-CS particles.

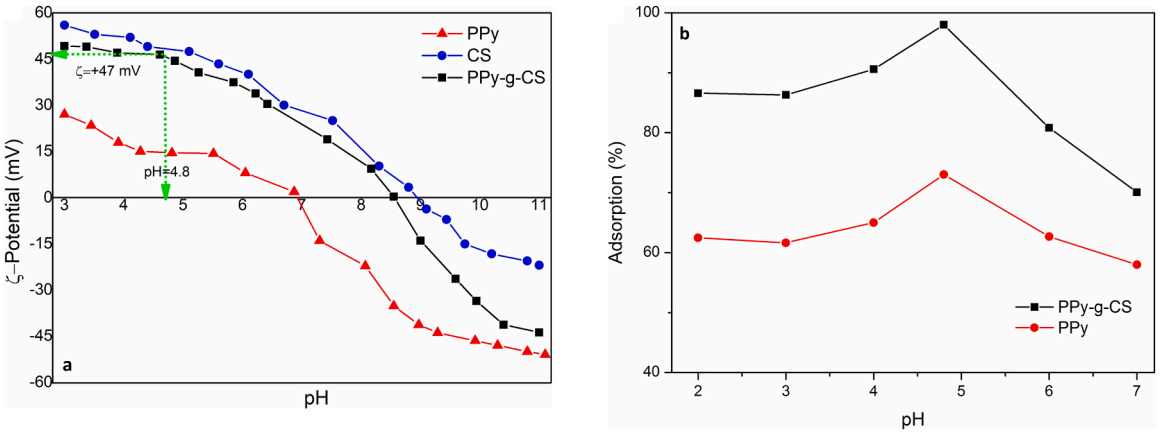

Fig. 2. (a) Change of ζ-potential as a function of pH for PPy, CS and PPy-*g*-CS. c_{sample} = 0.1 g/L, T = 25 °C. (b) The effect of pH on Cr(VI) removal efficiency for PPy and PPy-*g*-CS. $c_{adsorbent}$ = 2 g/L, 1.0×10^{-3} M Cr(VI) and T = 25 °C.

ζ-potential of the dispersion was also changed accordingly from + 56 mV to − 22 mV. In the literature, colloidal stability range of a dispersion is accepted as + 30 mV≤ ζ-potential≤ −30 mV at a certain pH values [29]. The nitrogen atoms of PPy, and –NH_2 groups of CS biopolymer were protonated at lower pH conditions than initial pH value, thus the more positive ζ-potential values were obtained for all the samples examined.

To better understand the surface properties of PPy-g-CS graft copolymer, basic electrokinetic properties were compared with the PPy homopolymer. The ζ-potential and IEP values of the copolymer were observed to shift to the more positive values. This may be attributed to the increased number of ionizable polycationic groups ($-NH_3^+$) on the PPy surfaces owing to the grafting with CS back-bone as shown in Fig. 1b, which may cause the enhanced electrostatic interactions between the copolymer surfaces and anionic forms of Cr(VI), thereby improving the adsorption performance of the PPy-*g*-CS biocompatible adsorbent.

The dominant Cr(VI) species vary, depending on the pH of the aqueous medium, as follows: H_2CrO_4 at pH< 1, $HCrO_4^-$ and $Cr_2O_7^{2-}$ at pH between 2 − 6, $Cr_2O_7^{2-}$ and CrO_4^{2-} at pH between 6 − 8, and CrO_4^{2-} at pH> 8 [30]. The adsorption experiments of PPy-*g*-CS dispersions were carried out at the initial pH of 4.8 which corresponds to the ζ-potential of + 47 mV, indicating that the particles were highly positively charged and colloidally stable ($\zeta_{PPy\text{-}g\text{-}CS} \geq +30$ mV). The Cr(VI) ions exist as $Cr_2O_7^{2-}$ and $HCrO_4^-$ forms at pH of 4.8. This pH value is very suitable to reach to the maximum Cr(VI) adsorptions on PPy-*g*-CS surfaces due to the increased interfacial electrostatic interactions.

3.3. Effect of pH on adsorption capacity

The pH value of a medium has a significant effect on the uptake of heavy metal by the adsorbents [27,31,32]. The percentage adsorption of Cr(VI) onto PPy and PPy-*g*-CS particles as a function of pH (2−7) is shown in Fig. 2b. The removal of Cr(VI) complex ions increased sharply at the optimum pH of 4.8 and slightly decreased with further increasing of pH between 4.8 and 7.0. The percentage uptake of Cr(VI) reached to 98 % with PPy-*g*-CS at the pH of 4.8 whereas PPy was only 73 % at the same pH. These ratios are in harmony with the ζ-potentials of PPy-*g*-CS and PPy as shown Fig. 2a. This increase in the electrostatic adsorption capacity may be attributed to the high ζ-potential of the PPy-*g*-CS copolymer due to its greater number of active functional adsorption sites. On the other hand, enhanced Cr(VI) adsorption at low pH was also reported and attributed to the high redox potential (1.33 eV) of $HCrO_4^-$ [33]. The decrease in the uptake rate of adsorption in the pH range of 4.8–7.0 may be attributed to the formation of gradually unprotonated amino groups present both in CS and PPy chains ($-NH_3^+ \leftrightarrow -NH_2$) [34].

At basic pH values, above the IEP, surface charges become negative for PPy-*g*-CS and PPy, and the concentration of free OH^- anions increase in the medium. On the other hand, the CrO_4^{2-} oxyanion has a reduction potential of − 0.26 eV indicating low electrostatic interactions with the adsorbents [33]. Therefore, pH of 4.8 is determined to be the optimum for adsorption of Cr(VI) onto PPy-*g*-CS for the rest of the experiments.

Further, when NaOH(aq) was added to increase the pH of the dispersion, $[H_3O^+]$ decreased and $[OH^-]$ increased. The initial ζ-potential of the PPy-*g*-CS colloidal dispersion shifted up to − 44 mV at pH of 11 due to the deprotonation of the protonated groups as shown in Fig. 2a. It was observed that, both the ζ-potential and Cr(VI) adsorption of PPy-*g*-CS decreased as the pH increased and vice versa. These results are in good agreement with the other studies reported in the literature on Cr (VI) adsorption with zwitterionic CS derivatives [35] and PPy/maghemite substrate [33].

Cr(VI) ions show varying oxidation states as the pH of the solutions changes. Thus, as the oxidation state of chromium ions change, their stability also changes. It is known that the most stable form of the chromium ion up to pH of 7 is $HCrO_4^-$. As the pH of the solution further increase lower oxidation states are detected [36,37]. The dominant chromium ion species in the medium was $HCrO_4^-$ ions at the maximum adsorption pH of 4.8, on the other hand, CrO_4^{2-} ion form was stable at higher pH values [38]. The ζ-potential also changes in a similar way. With the increasing valencies of the anions such as CrO_4^{2-} and SO_4^{2-} in dispersion, positive ζ-potentials of the particles decrease and shift to more negative values in the basic region. This is due to the presence of the Stern layer, which balances the positive surface charge created by the negatively charged divalent counter ions. The Debye length is one of the most important electrokinetic parameters and is a measure of the electrical double layer thickness (κ^{-1}). The κ^{-1} changes with the valency of ions in a colloidal dispersion by the following equation [39]:

$$\kappa^{-1} = \frac{0.3041}{Zc^{1/2}} \quad (4)$$

where, Z and c values indicate the valency and concentration of the ions in the dispersion, respectively. Accordingly, as the ion valence increases, the Debye length decreases and therefore the ζ-potential of the dispersion decreases [40]. In conclusion, with decreasing ζ-potential, the electrostatic interaction ability of PPy-*g*-CS decreases, so does the adsorption capacity which is in accordance with our initial hypothesis.

3.4. Effect of initial chromium concentration on adsorption capacity

The change of adsorbed Cr(VI) amount with initial Cr(VI) concentration at constant PPy and PPy-*g*-CS adsorbent amounts are investigated ($c_{adsorbent}$ = 2 g/L, contact time: 2 h, pH = 4.8 and T = 25 °C). It was

observed that, increasing initial concentration of Cr(VI), enhanced the uptake of Cr(VI) ions both by PPy and PPy-*g*-CS until a certain value then levelled off due to the saturation of the adsorbent surfaces (Fig. 3a). While a maximum removal of Cr(VI) was 0.38 mmol by PPy-*g*-CS at a constant adsorbent dose of 2 g/L, the maximum removal of Cr (VI) by PPy was found to be 0.27 mmol. Similar electrostatic adsorption behaviors of Cr(VI) ions (100 mg/L) are reported in the literature for CS-sodium tripolyphospahte beads as 15.23 mg/g and for CS/β-cyclodextrin/sodium tripolyphosphate beads as 15.64 for 100 mg/L Cr(VI) concentrations and concluding that as the initial concentration of Cr(VI) ions increase, so does the adsorption capacity of the adsorbent [34].

Positively charged surfaces of PPy-*g*-CS copolymer particles were covered gradually by the negatively charged $HCrO_4^-$ anions. Compared to PPy, the positively charged amino functional groups of PPy-*g*-CS increase in harmony with the increased ζ-potential and consequently interact with more $HCrO_4^-$ ions at the solution/adsorbent interface. It was observed that, when the concentration of Cr(VI) ions is lower than 0.005 mmol/L, there are adequate adsorption sites (-NH_2 groups) on the surfaces of PPy-*g*-CS copolymer for the uptake of Cr(VI) ions which is not the case when the Cr(VI) concentration exceeds 0.005 mmol/L due to the dominating electrostatic repulsive forces between the negatively charged $HCrO_4^-$ anions which resulted in the decreased uptake.

3.5. Effect of adsorbent dosage on adsorption capacity

PPy-*g*-CS exhibited higher adsorption rate (98 %) of Cr(VI) when compared with PPy (73 %) at the maximum adsorbent dosage of 0.1 g (4 g/L). The removal rate of PPy-*g*-CS enhanced from 56 % to 98 % as the amount of adsorbent increased 10 fold from 0.01 to 0.1 g. This may be attributed to the increased number of surface charges and number of cationic amino groups ($-NH_3^+$) as adsorption functional active sites of PPy-*g*-CS. When the PPy-*g*-CS dosage was greater than 0.05 g (2 g/L), Cr (VI) ions were almost completely drawn away from the solution. These results further confirmed that PPy-*g*-CS particles with enhanced positively surface charges exhibit excellent adsorption efficiency for Cr(VI) ions. Since the PPy-*g*-CS particles reached almost equilibrium after 2 g/L adsorbent dosage the rest of the experiment were carried out at this dosage. Similar adsorbent dosage effects were reported in the literature and the highest Cr(VI) removal efficiency of 97 % observed at 20 g/L of initial adsorbent dosage of chitosan/β-cyclodextrin beads [34]. Because of long reaction time, their adsorption studies were performed at low initial adsorbent concentration of 3.0 g/L.

3.6. Adsorption kinetics

Adsorption kinetics reveal the changes of adsorption rates in time by changing concentration or temperature at constant pressure. The variations of the amount of adsorption yield with different contact times are shown in Fig. 3c ($c_{adsorbent}$ = 2 g/L, 1.0 ×10^{-3} M Cr(VI), pH = 4.8 and T = 25 °C). It is clearly seen that the adsorption of Cr(VI) onto the both samples increased rapidly in the first 120 min due to the high inter-surface interactions between the PPy-*g*-CS particles and Cr(VI) anions ($HCrO_4^-$) and then levelled off. This may be attributed to the decreased number of non-interacting active groups on the adsorbents as the adsorption reaction approaches to the equilibrium state. The adsorption capacity (98 %) of PPy-*g*-CS was almost 1.5 times greater than PPy (73 %). This is may be due to the + 33 mV increase in the ζ-potential of PPy-*g*-CS (+47 mV at the pH of 4.8) with the active end amino groups on the

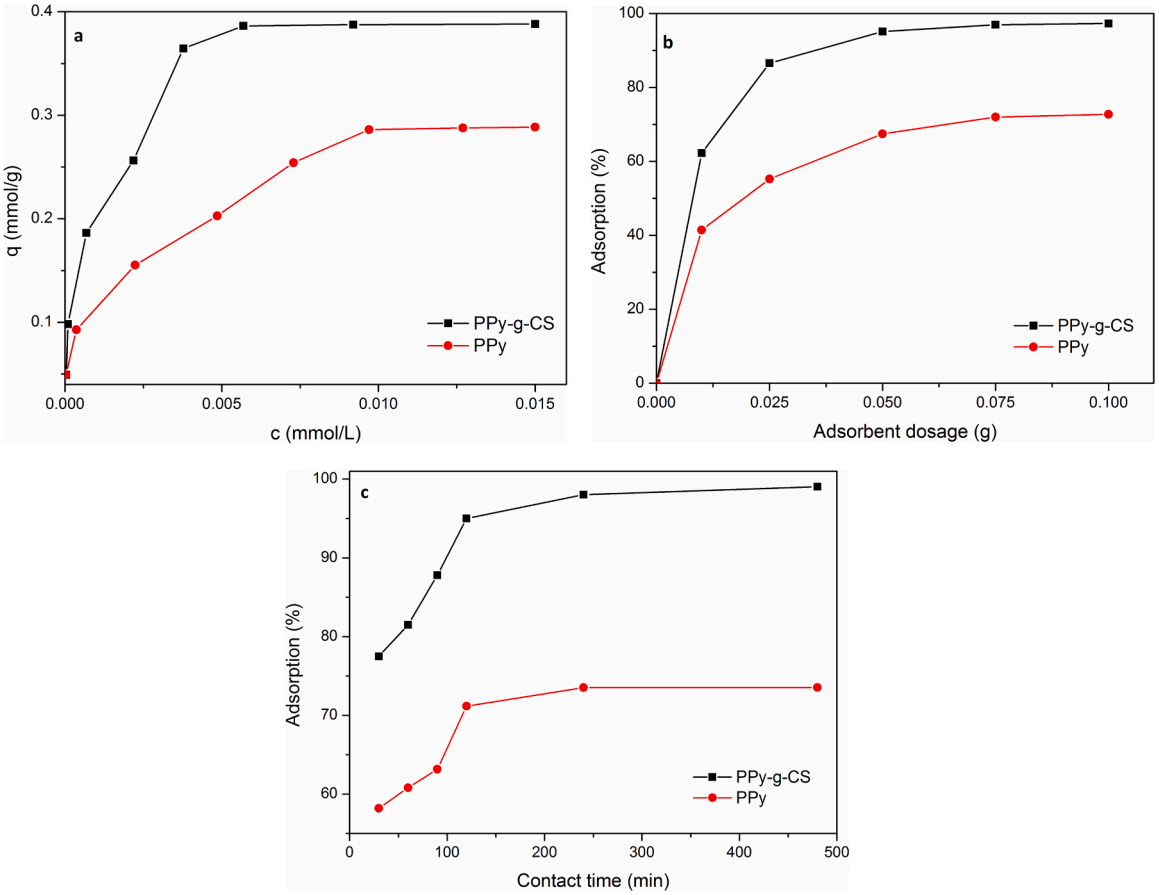

Fig. 3. (a) The effect of initial Cr(VI) concentration on Cr(VI) removal efficiency for PPy and PPy-*g*-CS adsorbents: $c_{adsorbent}$ = 2 g/L, contact time: 2 h, pH = 4.8 and T = 25 °C. (b) The effect of adsorbent dosage on Cr(VI) removal efficiency for PPy and PPy-*g*-CS, contact time: 2 h, [Cr(VI)] = 1.0 × 10^{-3} M, pH = 4.8 and T = 25 °C. (c) Effects of contact time on Cr(VI) removal efficiency for PPy and PPy-*g*-CS, pH = 4.8 and T = 25 °C.

CS chains when compared to the ζ-potential of pure PPy (+14 mV at the pH of 4.8).

Two models were used to evaluate the adsorption kinetic parameters of Cr(VI) on the PPy and PPy-*g*-CS particles, namely pseudo-first-order (PFO) and pseudo-second-order (PSO) models, and their linearized equations are given in Eqs. (5) and (6), respectively [41,42]:

$$\log(q_e - q_t) = \log q_e - \frac{k_1}{2.303}t \tag{5}$$

$$\frac{t}{qt} = \frac{1}{k_2 q_e^2} + \frac{1}{q}t \tag{6}$$

where, the amounts of Cr(VI) (mg/g) adsorbed at equilibrium and time t are shown as q_e and q_t, respectively. Pseudo-first-order and pseudo-second-order rate constants are shown as k_1 and k_2. Table 1 shows the two different kinetic model parameters of the PPy and PPy-*g*-CS samples. The correlation coefficient (R^2) of the pseudo-second-order kinetic model (0.999) for PPy-*g*-CS was higher than that of the pseudo-first-order kinetic model (0.891). In addition, the experimental values of q_e were observed to fit better to the pseudo-second-order kinetic model (Eq. 6) than the pseudo-first-order kinetic model (Eq. 5). Additionally, k_2 value of PPy-*g*-CS (0.121 g/mg min) was higher than PPy (0.111 g/mg min) which indicates faster uptake of Cr(VI) by PPy-*g*-CS than PPy. These results also support the pseudo-second-order kinetic model. Similar pseudo-second-order kinetic models were reported in the literature for PPy/MLS [4] and PPy/calcium rectorite composites [43]. Based on the positive increase in the ζ-potential of the PPy-*g*-CS copolymer particles, it is an important result that the driving force behind the Cr(VI) adsorption mechanism is the electrostatic interactions between $HCrO_4^-$ and $(-NH_3^+)$ions as reflected in Fig. 1b ($-NH_2 + H^+ \rightarrow -NH_3^+ \xrightarrow{HCrO_4^-} -NH_3^+HCrO_4^-$).

3.7. Adsorption isotherms

The Freundlich and Langmuir models are applied to fit the adsorption isotherm data. Freundlich isotherm proposes a non-linear and a monolayer sorption model by taking the inhomogeneous energy distributions of the active groups and the take interactions between the adsorbed species into account as described in Eq. (7):

$$q_e = K_F C_e^{1/n} \tag{7}$$

where, K_F (mmol/g) and n are the adsorption capacity and adsorption intensity, respectively.

On the other hand, the Langmuir model proposes that adsorption of colloidal adsorbate ions take place as monolayer on the substrate but does not take the interactions between the adsorbed molecules into account. It suggests that there are uniform adsorption energies on the adsorbent surface and that the transmigration of the adsorbate will not be possible as described in Eq. (8):

$$q_e = \frac{Q_L b C_e}{1 + bC_e} \tag{8}$$

where, Q_L (mmol/g) is the Langmuir capacity of adsorption and *b* is the energy of adsorption. Another analysis of the Langmuir model can be performed based on R_L, which is known as both a separation factor and a dimensionless equilibrium parameter, as shown in Eq. (9).

$$R_L = \frac{1}{1 + bc_0} \tag{9}$$

where, *b* (L·mg^{-1}) and c_0 (mg·L^{-1}) are the constant of Langmuir and the highest initial concentration of metal ions, respectively. Whether the adsorption of the adsorbate species is favored or not, is defined by the changing value of R_L: It is mentioned in the literature that if $0 < R_L < 1$ adsorption of adsorbate onto the substrate surface is favored. If $R_L > 1$ the adsorption is un-favored, if $R_L = 1$ it is linear adsorption and if $R_L = 0$ adsorption is irreversible [44–46].

The Freundlich and Langmuir adsorption isotherms for the PPy and the PPy-*g*-CS copolymer are shown in Fig. 4a-b, respectively and the isotherm parameters are tabulated in Table 2. For PPy and PPy-*g*-CS copolymer, the R^2 values of the Freundlich model (0.981 for PPy and 0.974 for PPy-*g*-CS) were much higher than the Langmuir model (0.933 for PPy and 0.968 for PPy-*g*-CS). The values showed that the Cr(VI) adsorption process onto the both sample surfaces were better fitted to the Freundlich isotherm. Furthermore, the maximum adsorption capacity $K_F = 128.48$ mg/g at 25 °C with an affinity value $n = 2.65$ represents an effective adsorption of Cr(VI) onto the PPy-*g*-CS copolymer particles. The maximum adsorption capacities of some adsorbents based on PPy and CS reported in the literature are tabulated in Table 3 for comparison. It is clearly seen that the adsorption capacity of PPy-*g*-CS graft copolymer has medium effect and is higher than most of the adsorbents listed in Table 3. According to the values obtained from Langmuir isotherms as tabulated in Table 2, R_L value is between 0 and 1, confirming that the adsorption process of PPy-*g*-CS is very favorable. Also, the 1/n parameter in the Freundlich model was found to be between 0.1 and 0.5, which shows that adsorption is easy [46]. On the other hand, Langmuir model is reported to well fit to the adsorption isotherms of Cr(IV) ions onto PPy/MLS [4], cross-linked CS and CS/β-cyclodextrin beads [34], PPy/calcium rectorite composite [44] and CS flakes [49].

The Dubinin-Radushkevitch (D-R) model has been the fundamental model to quantitatively describe the adsorption of gases and vapors by microporous sorbents [61]. The D-R isotherm model can be applied to distinguish between physical and chemical adsorption [62,63]. It is proposed by the theory that when the adsorption energy (*E*) value is between 1 and 16 kJ/mol it can be used to determine the adsorption mechanism. If $E < 8$, it is described as physisorption [63]. From this point of view, the D-R parameters are also calculated and tabulated in Table 2. With high correlation coefficients ($R^2 > 0.98$), experimental results are in agreement with the D-R isotherm model. The magnitude of *E* was found to be 3.53 kJ/mol, indicating that the Cr(VI) adsorption mechanism onto PPy-*g*-CS is by physisorption.

3.8. Thermodynamics parameters

The influence of temperature on Cr(VI) adsorption was investigated between 25 and 65 °C. It was observed that while the adsorption of Cr (VI) onto PPy was slow, the adsorption of Cr(VI) onto PPy-*g*-CS slightly increased with rising temperature (Fig. 4c). When the variation of ζ-potential with temperature was examined, the ζ-potential of the PPy-*g*-CS particles exhibited little change despite the increase in temperature. Temperature has a significant effect on some parameters of a dispersion

Table 1
Adsorption kinetic parameters.

	Adsorbent	Pseudo first order (PFO)				Pseudo second order (PSO)			
		k_1 (1/min)	$q_{e\ (exp)}$ (mg/g)	$q_{e\ (cal)}$ (mg/g)	R^2	k_2 (g/mg.min)	$q_{e\ (exp)}$ (mg/g)	$q_{e\ (cal)}$ (mg/g)	R^2
Cr (VI)	PPy-*g*-CS	0.366	0.495	0.116	0.891	0.121	0.495	0.498	0.999
	PPy	0.231	0.334	0.240	0.873	0,111	0.334	0.363	0.999

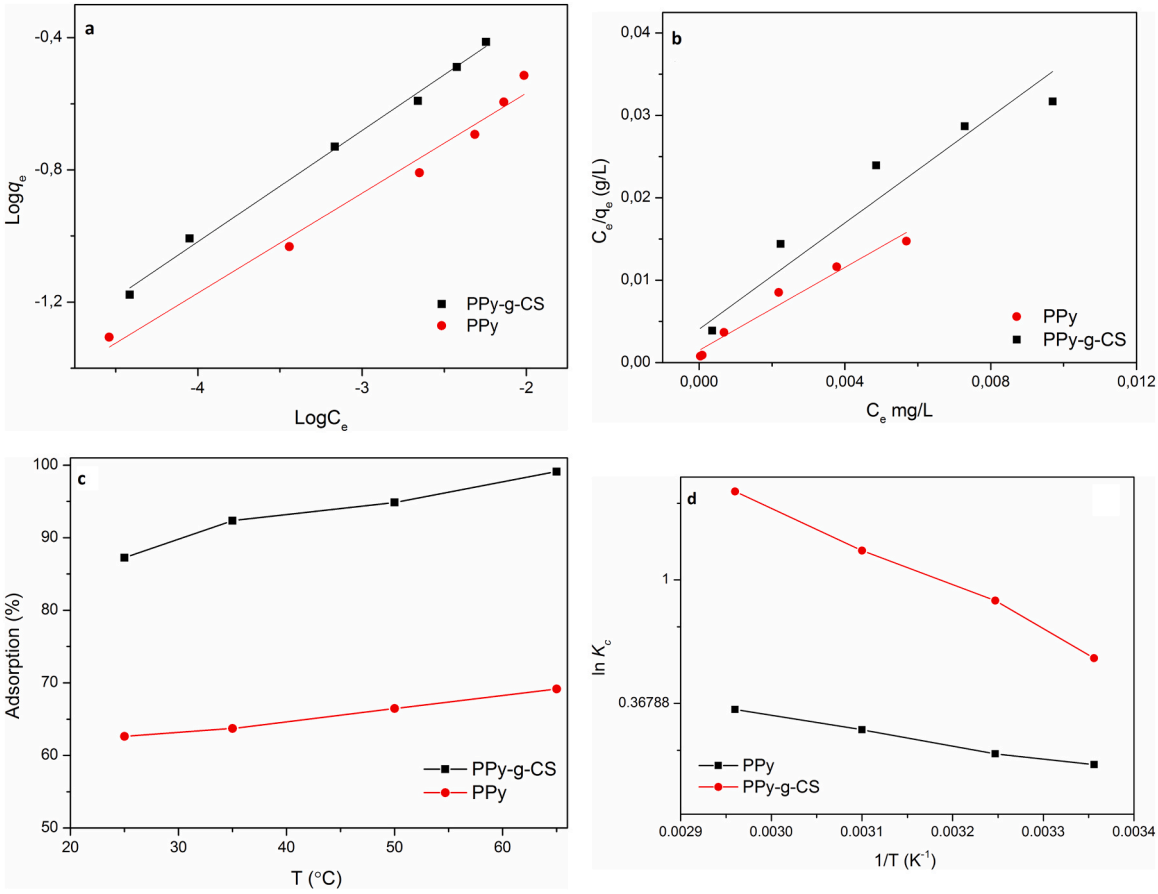

Fig. 4. (a) Freundlich and (b) Langmuir Adsorption isotherms for Cr(VI) on the PPy and PPy-*g*-CS. (c) Effect of temperature on Cr(VI) removal efficiency. (d) Plot to determine thermodynamic parameters for PPy and PPy-*g*-CS, pH= 4.8.

Table 2
Freundlich, Langmuir and Dubinin-Radushkevic (D-R) adsorption isotherm parameters at 298 K.

Freundlich adsorption isotherm					
	Adsorbent	K_F (mmol\g)	n	R^2	1\n
Cr (VI)	PPy-*g*-CS	0.4368	2.648	0.974	0.377
	PPy	0.0369	3.306	0.981	0.302
Langmuir adsorption isotherm					
		Q (mmol\g)	b L\ mmol	R^2	R_L
Cr (VI)	PPy-*g*-CS	0.499	1336.00	0.968	0.42
	PPy	0.310	806.45	0.933	0.55
Dubinin- Radushkevich adsorption isotherm					
		q_e (mmol\g)	K_{D-R} (mol^2\kJ^2)	E kJ\mol	R^2
Cr (VI)	PPy-*g*-CS	7.269	0.00000004	3.53	0.980
	PPy	9.130	0.00000004	3.53	0.985

Table 3
Comparison of the Cr(VI) removing capasities of PPy-g-CS and some reported adsorbents at 25 °C.

Adsorbent	Adsorption capacity, q_m (mg/g)	Optimum pH	Reference
Quaternized chitosan microspheres	39.11	5.0	[46]
PPy/montmorillonite clay nanocomposite	119.3	2.0	[47]
Magnetic cyclodextrin–chitosan	67.66	2.0	[48]
Chitosan flakes	22.09	3.0	[49]
Polypyrrole/Fe_3O_4	169.5	2.0	[50]
Polypyrrole/wood sawdust	3.4	5.0	[51]
Polyacrilonitrile/PPy core/shell mats	61.8	2.0	[52]
Polypyrrole-poyaniline nanofibers	227	2.0	[53]
Chitosan	110.5	4.0	[54]
Polypyrrole-halloysite nanotube halloysite nanotube clay	149.5	2.0	[55]
Chitosan microfibers	112.5	5.0	[56]
Crosslinked chitosan	325.2	2.0	[57]
Polypyrrole/maghemite magnetic	209.0	2.0	[58]
Nano Fe oxide/chitosan beads	69.8	5.0	[59]
Maghemite/Chitosan/ Polypyrrole NC	301.2	2.0	[60]
PPy-*g*-CS graft copolymer	128.48	4.8	Present study

such as dielectric constant, viscosity, ion adsorption, thermal energy and desorption [2]. Electrophoretic mobility of the adsorbent particles raise with increasing temperature as a result of their enhanced kinetic energies, increased ionic mobility and decreased viscosity of the medium [63], which undergoes to the weakened formation of the diffuse layer and results in the variations in ζ-potentials [64].

Thermodynamic parameters of the samples, such as Gibbs free energy change (ΔG°), standard enthalpy change (ΔH°) and standard entropy change (ΔS°) were calculated from the slope of the Van't Hoff plot of $\ln K_c$ vs. 1/T for four different temperatures (Fig. 4d) and results obtained are tabulated in Table 4. The positive values of ΔH° indicates that the nature of Cr(VI) adsorption process is endothermic ($\Delta H°_{PPy}$ = 6.20 kJ/mol, $\Delta H°_{PPy\text{-}g\text{-}CS}$ = 7.12 kJ/mol). This may be due to the raised thermal energies of the adsorbate ions with rising temperature of the

Table 4
Thermodynamic parameters for the samples.

T (K)		PPy-*g*-CS				PPy			
		ΔG° (kj/mol)	ΔH° (kj/mol)	ΔS° (kj/mol.K)	TΔS° (kj/mol)	ΔG° (kj/mol)	ΔH° (kj/mol)	ΔS° (kj/mol.K)	TΔS° (kj/mol)
Cr (VI)	298	-1.293	7.117	0.247	72.570	-0.546	6.204	0.025	7.319
	308	-2.165			76.283	-0.626			7.693
	323	-3.401			79.996	-0.798			8.068
	338	-5.749			83.710	-0.985			8.442

system and ends up with the enhanced adsorption affinity of the functional surfaces. The ΔG° values are negative and decreases with the increase in temperature, which illustrated the increased spontaneity and feasibility of adsorption at all the temperatures [65]. In addition, the ΔS° of PPy and the PPy-*g*-CS copolymer was 25 and 247 J/mol K, respectively and indicating that the system exhibited increasing randomness during adsorption processes.

3.9. Reusability assays

Variations of Cr(VI) removal efficiencies with PPy-*g*-CS copolymer adsorbent after five times of repeated adsorption-desorption processes are depicted in Fig. 5. The uptake percentage of the adsorbent gradually decreased with increasing cycles of adsorption processes. The removal efficiencies of cycles from 1 to 5 were found to be 98 %, 98 %, 95 %, 90 % and 87 %, respectively. This decrease in the adsorption efficiency of the functional adsorbents is attributed to the degradation of polymer chains due to the interactions with Cr(VI) ions during the repeated loading cycles which undergoes to the formation of shorter active sites on the adsorbent surfaces [66].

3.10. Adsorption mechanism of Cr(VI)

The mechanism of Cr(VI) uptake from the solution by PPy-*g*-CS graft copolymer particles are schematically shown in Fig. 1b. According to the Fig. 1b, the PPy particles were not colloidally stable due to low positive ζ-potential value (+14 mV at pH of 4.8) at acidic conditions. This low positive ζ-potential can be attributed to the N^+ sites in the pyrrole monomer structure [26]. On the other hand, after grafting of PPy with positively charged polycationic CS chains, positive ζ-potential value of the PPy-*g*-CS copolymer increased to + 47 mV at pH of 4.8 due to $-NH_3^+$ groups of CS. In addition, owing to the increased ζ-potential, colloidal stability of PPy-*g*-CS graft copolymer particles in the dispersion increased.

When chromium ions are added to the PPy-*g*-CS(aq) colloidal dispersion system at low pH values (by adding HCl), the $HCrO_4^-$ ions are attracted to.

$-NH_3^+$ by electrostatic interactions. In addition, $HCrO_4^-$ ions displacement with OH^- and Cl^- ions occur. Thus, more $HCrO_4^-$ adsorption on the PPy-*g*-CS copolymer take place. At high pH values (by adding NaOH), desorption process occurs and OH^- ions exchange with adsorbed $HCrO_4^-$ ions. Similar adsorption and desorption processes were reported in the literature for CS/β-cyclodextrin beads [48] and PPy/Polyaniline nanofibers [53].

4. Conclusion

The ζ-potential (+47 mV at pH of 4.8) of biodegradable PPy-*g*-CS graft copolymer particles was enhanced due to the synergistic effect of polycationic PPy and CS units. The adsorption capacity of PPy-*g*-CS was enhanced approximately 1.5 times, owing to the increased ζ-potential from + 14 mV (PPy) to + 47 mV (PPy-*g*-CS) at the initial pH of 4.8. The ζ-potential value and Cr(VI) adsorption capacity of the PPy-*g*-CS graft copolymer particles changed in harmony. The maximum chromium ions adsorption with 98 % of the PPy-*g*-CS copolymer was occurred due to the

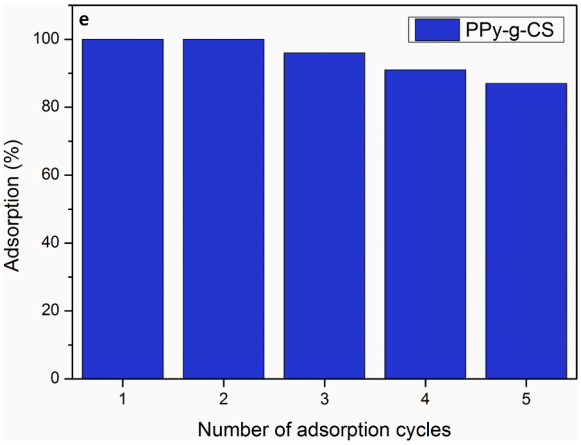

Fig. 5. Adsorption/desorption cycles of Cr(VI) onto PPy-*g*-CS particles.

electrostatic attractions between $-NH_3^+$ and $HCrO_4^-$ ions at the pH of 4.8 indicating positive ζ-potential of the PPy-*g*-CS ($\zeta_{pH=4.8} = +47$ mV). Adsorption kinetics followed a pseudo-second-order kinetic model and Freundlich isotherm was better fitted. The maximum adsorption capacity was $K_F = 128.48$ mg/g at 25 °C. The mechanism of Cr(VI) adsorption by PPy-*g*-CS was physisorption and the driving force is electrostatic interactions since the *E* value in the D-R isotherm was < 8 kJ/mol. According to thermodynamic parameters, adsorption process is spontaneous and endothermic. In conclusion, biodegradable PPy-*g*-CS graft copolymer with enhanced positive ζ-potential can be an environmentally friendly and new adsorbent candidate for the withdrawal of negatively charged pollutant ions from wastewater resources.

CRediT authorship contribution statement

Murat Oztas: Methodology, Investigation, Writing – original draft. **Mehmet Cabuk:** Conceptualization, Methodology, Investigation, Writing – original draft. **Fethiye Gode:** Conceptualization, Methodology, Investigation. **Halil Ibrahim Unal:** Conceptualization, Methodology, Writing – review & editing. **Mustafa Yavuz:** Methodology, Writing – review & editing.

Declaration of Competing Interest

The authors declare that they have no known competing financial interests or personal relationships that could have appeared to influence the work reported in this paper.

Data availability

Data will be made available on request.

Acknowledgements

The authors would like to thank Mersin University Scientific Research Projects Unit [Project no: 2021-1-AP4-4376]; and COST

Actions Greenering, CA18224 and Priority, CA20101 supported by COST (European Cooperation Science and Technology).

References

[1] J. Chen, M. Yu, C. Wang, J. Feng, W. Yan, Insight into the synergistic effect on selective adsorption for heavy metal ions by a polypyrrole/TiO_2 composite, Langmuir 34 (2018) 10187–10196.

[2] N.H. Kera, M. Bhaumik, N. Ballav, K. Pillay, S.S. Ray, A. Maity, Selective removal of Cr(VI) from aqueous solution by polypyrrole/2,5-diaminobenzene sulfonic acid composite, J. Colloid Interface Sci. 476 (2016) 144–157.

[3] V. Neagu, S. Mikhalovsky, Removal of hexavalent chromium by new quaternized crosslinked poly(4-vinylpyridines), J. Hazard. Mater. 183 (2010) 533–540.

[4] L. Du, P. Gao, Y. Meng, Y. Liu, S. Le, C. Yu, Highly efficient removal of Cr(VI) from aqueous solutions by polypyrrole/monodisperse latex spheres, ACS Omega 5 (2020) 6651–6660.

[5] WHO, Guidelines for Drinking-water Quality, fourth ed., World Health Organization, Geneva, Switzerland, 2011.

[6] S. Sharma, D. Pathania, P. Singh, Preparation, characterization and Cr(VI) adsorption behavior study of poly(acrylic acid) grafted Ficus carica bast fiber, Adv. Mater. Lett. 4 (2013) 271–276.

[7] S. Vasudevan, J. Lakshmi, G. Sozhan, Simultaneous removal of Co, Cu, and Cr from water by electrocoagulation, Toxicol. Environ. Chem. 94 (2012) 1930–1940.

[8] R. Karthik, S. Meenakshi, Removal of Pb(II) and Cd(II) ions from aqueous solution using polyaniline grafted chitosan, J. Chem. Eng. 263 (2015) 168–177.

[9] A.L.P.F. Caroni, C.R.M. de Lima, M.R. Pereira, J.L.C. Fonseca, Tetracycline adsorption on chitosan: a mechanistic description based on mass uptake and zeta potential measurements, Colloid Surf. B 100 (2012) 222–228.

[10] S. Pandey, S.B. Mishra, Organic-inorganic hybrid of chitosan/organoclay bionanocomposites for hexavalent chromium uptake, J. Colloid Interface Sci. 361 (2011) 509–520.

[11] N. Ballav, H.J. Choi, S.B. Mishra, A. Maity, Synthesis, characterization of Fe_3O_4@ glycine doped polypyrrole magnetic nanocomposites and their potential performance to remove toxic Cr(VI), J. Ind. Eng. Chem. 20 (2014) 4085–4093.

[12] S.H. Huang, D.H. Chen, Rapid removal of heavy metal cations and anions from aqueous solutions by an amino-functionalized magnetic nano-adsorbent, J. Hazard. Mater. 163 (2009) 174–179.

[13] T. Dai, M. Tanaka, Y.Y. Huang, M.R. Hamblin, Chitosan preparations for wounds and burns: antimicrobial and wound-healing effects, Expert Rev. Anti Infect. Ther. 9 (2011) 857–879.

[14] A.T. Ramaprasad, V. Rao, G. Sanjeev, S.P. Ramanani, S. Sabharwal, Grafting of polyaniline onto the radiation crosslinked chitosan, Synth. Met.. 159 (2009) 1983–1990.

[15] B. Samiey, C.H. Cheng, J. Wu, Organic-inorganic hybrid polymers as adsorbents for removal of heavy metal ions from solutions: a review, Materials 7 (2014) 673–726.

[16] F.T.R. Almeida, B.C.S. Ferreira, A.L.S.L. Moreira, R.P. Freitas, L.F. Gil, L.V. A. Gurgel, Application of a new bifunctionalized chitosan derivative with zwitterionic characteristics for the adsorption of Cu^{2+}, Co^{2+}, Ni^{2+}, and oxyanions of Cr^{6+} from aqueous solutions: kinetic and equilibrium aspects, J. Colloid Interface Sci. 466 (2016) 297–309.

[17] V.K. Mourya, N.N. Inamdar, Chitosan-modifications and applications: opportunities galore, React. Funct. Polym. 68 (2008) 1013–1051.

[18] S.K. Kumar, C.U. Kumar, V. Rajesh, N. Rajesh, Microwave assisted preparation of n-butylacrylate grafted chitosan and its application for Cr(VI) adsorption, Int. J. Biol. Macromol. 66 (2014) 135–143.

[19] N.A. Negm, R. El Sheikh, A.F. El-Farargy, H.H.H. Hefni, M. Bekhit, Treatment of industrial wastewater containing copper and cobalt ions using modified chitosan, J. Ind. Eng. Chem. 21 (2015) 526–534.

[20] G.Z. Kyzas, P.I. Siafaka, D.A. Lambropoulou, N.K. Lazaridis, D.N. Bikiaris, Poly (itaconic acid)-grafted chitosan adsorbents with different cross-linking for Pb(II) and Cd(II) uptake, Langmuir 40 (2014) 120–131.

[21] X. Guo, G.T. Fei, H. Su, L.D. Zhang, Synthesis of polyaniline micro/nanospheres by a copper(II)-catalyzed self assembly method with superior adsorption capacity of organic dye from aqueous solution, J. Mater. Chem. 21 (2011) 8618–8625.

[22] X. Lu, Z. Qiu, Y. Wan, Z. Hu, Y. Zhao, Preparation and characterization of conducting polycaprolactone/chitosan/polypyrrole composites, Compos. Part A Appl. Sci. Manuf. 41 (2010) 1516–1523.

[23] S. Temmel, W. Kern, T. Luxbacher, Zeta potential of photochemically modified polymer surfaces, Prog. Colloid Polym. Sci. 132 (2006) 54–61.

[24] X. Zhang, R. Bai, Surface electric properties of polypyrrole in aqueous solutions, Langmuir 19 (2003) 10703–10709.

[25] W.L. Du, Y.L. Xu, Z.R. Xu, C.L. Fan, Preparation, characterization and antibacterial properties against E. coli K88 of chitosan nanoparticle loaded copper ions, Nanotechnology 19 (2008) 85707–85711.

[26] M. Cabuk, M. Yavuz, H.I. Unal, Colloidal, electrorheological, and viscoelastic properties of polypyrrole-graft-chitosan biodegradable copolymer, J. Intel. Mater. Syst. Str. 26 (2015) 1799–1810.

[27] R.J. Lee, R. Temmer, T. Tamm, A. Aabloo, R. Kiefer, Renewable antioxidant properties of suspensible chitosan–polypyrrole composites, React. Funct. Polym. 73 (2013) 1072–1077.

[28] M. Cabuk, Y. Alan, H.I. Unal, Enhanced electrokinetic properties and antimicrobial activities ofbiodegradable chitosan/organo-bentonite composites, Carbohydr. Polym. 161 (2017) 71–81.

[29] J. Tan, Y. Song, X. Huang, L. Zhou, Facile functionalization of natural peach gum polysaccharide with multiple amine groups for highly efficient removal of toxic hexavalent chromium (Cr(VI)) ions from water, ACS Omega 3 (2018) 17309–17318.

[30] Y. Lei, X. Qian, J. Shen, X. An, Integrated reductive/adsorptive detoxification of Cr (VI)-contaminated water by polypyrrole/cellulose fiber composite, Ind. Eng. Chem. Res. 51 (2012) 10408–10415.

[31] S. Deng, R. Bai, Removal of trivalent and hexavalent Cr with aminated polyacrylonitrile fibers: performance and mechanisms, Water Res. 38 (2004) 2424–2432.

[32] I. Ghorbel-Abid, C. Vagner, R. Denoyel, M. Trabelsi-Ayadi, Effect of cadmium and chromium adsorption on the zeta potential of clays, Desalin. Water Treat. 57 (2016) 17128–17138.

[33] A.L. Chavez-Guajardo, J.C. Medina-Llamas, L. Maqueira, C.A.S. Andrade, K.G. B. Alves, C.P.D. Melo, Efficient removal of Cr(VI) and Cu(II) ions from aqueous media by use of polypyrrole/maghemite and polyaniline/maghemite magnetic nanocomposites, Chem. Eng. J. 281 (2015) 826–836.

[34] T. Kekes, G. Kolliopoulos, C. Tzia, Hexavalent chromium adsorption onto crosslinked chitosan and chitosan/β-cyclodextrin beads: novel materials for water decontamination, J. Environ. Chem. Eng. 9 (2021), 105581.

[35] P. Xu, G. Bajaj, T. Shugg, W.G. Van Alstine, Y. Yeo, Zwitterionic chitosan derivatives for pH-sensitive stealth coating, Biomacromolecules 11 (2010) 2352–2358.

[36] F. Gode, E. Moral, Column study on the adsorption of Cr(III) and Cr(VI) using Pumice, Yarıkkaya brown coal, Chelex-100 and Lewatit MP 62, Bioresour. Technol. 99 (2008) 1981–1991.

[37] V. Sarin, K.K. Pant, Removal of Cr from industrial waste by using eucalyptus bark, Bioresour. Technol. 97 (2006) 15–20.

[38] R. Karthik, S. Meenakshi, Chemical modification of chitin with polypyrrole for the uptake ofPb(II) and Cd(II) ions, Int. J. Biol. Macromol. 78 (2015) 157–164.

[39] A. Kitahara, Electrical phenomena at interfaces: fundamentals, in: A. Watanabe (Ed.), Measurements and Applications, Marcel Dekker, New York, 1984.

[40] M. Cabuk, M. Yavuz, H.I. Unal, Y. Alan, Synthesis, characterization, and enhanced antibacterial activity of chitosan-based biodegradable conducting graft copolymers, Polym. Compos. 36 (2014) 497–503.

[41] A. Gok, F. Gode, B. Esencan Turkaslan, Chromium(VI) ion removal from solution by polyaniline/pumice composite, Asian J. Chem. 19 (2007) 3023–3034.

[42] K.Z. Elwakeel, removal of Cr(VI) from alkaline aqueous solutions using chemically modified magnetic chitosan resins, Desalination 250 (2010) 105–112.

[43] Y. Xu, J. Chen, R. Chen, P. Yu, S. Guo, X. Wang, Adsorption and reduction of chromium(VI) from aqueous solution using polypyrrole/calcium rectorite composite adsorbent, Water Res. 160 (2019) 148–157.

[44] A. Gallo-Cordova, M.P. Morales, E. Mazarío, Effect of the surface charge on the adsorption capacity of chromium(VI) of iron oxide magnetic nanoparticles prepared by microwave-assisted synthesis, Water 11 (2019) 2372–2383.

[45] T.W. Weber, R.K. Chackravorti, Pore and solid diffusion models for fixed bed adsorber, J. Am. Inst. Chem. Eng. 20 (1974) 228–238.

[46] C. Hua, R. Zhang, F. Bai, P. Lu, X. Liang, Removal of chromium (VI) from aqueous solutions using quaternized chitosan microspheres, Chin. J. Chem. Eng. 25 (2017) 153–158.

[47] K.Z. Setshedi, M. Bhaumik, S. Songwane, M.S. Onyango, A. Maity, Exfoliated polypyrrole-organically modified montmorillonite clay nanocomposite as a potential adsorbent for Cr(VI) removal, Chem. Eng. J. 222 (2013) 186–197.

[48] L. Li, L. Fan, M. Sun, H. Qiu, X. Li, H. Duan, C. Luo, Adsorbent for chromium removal based on graphene oxide functionalized with magnetic cyclodextrin–chitosan, Colloids Surf. B 107 (2013) 76–83.

[49] Y.A. Aydin, N.D. Aksoy, Adsorption of chromium on chitosan: optimization, kinetics and thermodynamics, Chem. Eng. J. 151 (2009) 188–194.

[50] M. Bhaumik, A. Maity, V.V. Srinivasu, M.S. Onyango, Enhanced removal of Cr(VI) from aqueous solution using polypyrrole/Fe3O4 magnetic nanocomposite, J. Hazard. Mater. 190 (1) (2011) 381–390.

[51] R. Ansari, N.K. Fahim, Application of polypyrrole coated on wood sawdust for removal of Cr(VI) ion from aqueous solutions, React. Funct. Polym. 67 (2007) 367–374.

[52] J. Wang, K. Pan, Q. He, B. Cao, Polyacrylonitrile/Polypyrrole core/shell nanofiber mat for the removal of hexavalent chromium from aqueous solution, J. Hazard. Mater. 244–245 (2013) 121–129.

[53] M. Bhaumik, A. Maity, V.V. Srinivasu, M.S. Onyango, Removal of hexavalent chromium from aqueous solution using polypyrrole-polyaniline nanofibers, Chem. Eng. J. 181–182 (2012) 323–333.

[54] Y. Abatneh, O. Sahu, Removal of chromium by biosorption method (Chitosan), Int. Lett. Nat. Sci. 8 (2014) 44–55.

[55] N. Ballav, H.J. Choi, S.B. Mishra, A. Maity, Polypyrrole-coated halloysite nanotube clay nanocomposite: synthesis, characterization and Cr(VI) adsorption behaviour, Appl. Clay Sci. 102 (2014) 60–70.

[56] A.M. Abdel-Mohsen, J. Jancar, L. Kalina, A.F. Hassan, Comparative study of chitosan and silk fibroin staple microfibers on removal of chromium (VI): fabrication, kinetics and thermodynamic studies, Carbohydr. Polym. 234 (2020), 115861.

[57] M. Vakili, S. Deng, T. Li, W. Wang, W. Wang, G. Yu, Novel crosslinked chitosan for enhanced adsorption of hexavalent chromium in acidic solution, Chem. Eng. J. 347 (2018) 782–790.

[58] A.E. Chavez-Guajardo, J.C. Medina-Llamas, L. Maqueira, C.A.S. Andrade, K.G. B. Alves, C.P. de Melo, Efficient removal of Cr (VI) and Cu (II) ions from aqueous media by use of polypyrrole/maghemite and polyaniline/maghemite magnetic nanocomposites, Chem. Eng. J. 281 (Suppl. C) (2015) 826–836.

[59] J. Lu, K. Xu, J. Yang, Y. Hao, F. Cheng, Nano iron oxide impregnated in chitosan bead as a highly efficient sorbent for Cr(VI) removal from water, Carbohydr. Polym. 173 (2017) 28–36.
[60] E.S. Reis, F.D.S. Gorza, G.C. Pedro a, B.G. Maciel, R.J. Silva, G.P. Ratkovski, C. P. Melo, (Maghemite/Chitosan/Polypyrrole) nanocomposites for the efficient removal of Cr (VI) from aqueous media, J. Environ. Chem. Eng. 9 (2021), 104893.
[61] N.D. Hutson, R.T. Yang, Theoretical basis for the Dubinin-Radushkevitch (D-R) adsorption isotherm equation, Adsorption 3 (1997) 189–195.
[62] J. Lin, Y. Zhan, Z. Zhu, Adsorption characteristics of copper (II) ions from aqueous solution onto humic acid-immobilized surfactant-modified zeolite, Colloids Surf. A Physicochem. Eng. 384 (2011) 9–16.
[63] W.S. Wan Ngah, S. Fatinathan, Adsorption characterization of Pb(II) and Cu(II) ions onto chitosan-tripolyphosphate beads: kinetic, equilibrium and thermodynamic studies, J. Environ. Manag. 91 (2010) 958–969.
[64] M. Cabuk, M. Yavuz, H.I. Unal, Electrokinetic, electrorheological and viscoelastic properties of polythiophene-graft-Chitosan copolymer particles, Colloids Surf. A Physicochem. Eng. 510 (2016) 231–238.
[65] M. Bhaumik, S. Agarwal, V.K. Gupta, A. Maity, Enhanced removal of Cr(VI) from aqueous solutions using polypyrrole wrapped oxidized MWCNTs nanocomposites adsorbent, J. Colloid Interface Sci. 470 (2016) 257–267.
[66] Y. Xu, J. Chen, R. Chen, P. Yu, S. Guo, X. Wang, Adsorption and reduction of chromium(VI) from aqueous solution using polypyrrole/calcium rectorite composite adsorbent, Water Res. 160 (2019) 148–157.